

# Radar wind profiler observations of solar semidiurnal atmospheric tides

C. David Whiteman and X. Bian

Pacific Northwest Laboratory, Richland, Washington

**Abstract.** Semidiurnal solar tides in the mid-latitude troposphere are investigated using harmonic analysis of 404 MHz radar profiler wind data obtained from a wide longitude zone in the U.S. The tides are apparent above a 1000-m-deep surface layer and increase in amplitude with height, attaining speeds of 0.5-0.7 m/s at 5-7 km. Observed wind characteristics agree well with tidal characteristics obtained with a dynamical model driven by observed global semidiurnal horizontal pressure gradients.

## 1. Introduction

Solar tides are major aeronomic features of the earth's upper atmosphere (Chapman and Lindzen, 1970), but their effects in the troposphere are more subtle and have received far less attention from geophysicists and atmospheric scientists. The development and deployment of vertically-pointing, continuously-operating pulsed Doppler wind profiling radars provides a new tool that may be applied to the observation of tides in the lower atmosphere. These instruments provide vertical profiles of winds that are averaged over 1-h in a fixed atmospheric volume, and provide much better time resolution than has been available until now for the observation of semidiurnal wind systems. In this paper, we use observations from three radar profilers to determine semidiurnal tropospheric tidal characteristics at mid-latitude sites in North America.

## 2. Radar Profilers and Data Analysis

Pulsed Doppler radar wind profilers are now in widespread use in the U.S., having been developed in the 1980s for meteorological applications by the National Oceanic and Atmospheric Administration's Aeronomy and Wave Propagation Laboratories. Wind profilers and their operating characteristics have been described by Doviak and Zrnic (1984) and data processing procedures have been described by Strauch et al. (1984). The data used in this paper are vertical profiles of hour-averaged horizontal winds within fixed vertical layers or "range gates" from continuously operating, unattended, three-beam 404-MHz radar wind profilers operated in the high-altitude, coarse range resolution mode. Data are hour averages over 250-m range gates beginning with the layer centered at 500 m AGL. Because radar beam scattering from migrating birds is known to contaminate radar profiler wind data (Wilczak et al., 1995), we have focused our analyses entirely on the winter season when migrations are at a minimum. The profiler locations and periods of record are provided in Table 1 and Figure 1.

Copyright 1995 by the American Geophysical Union.

Paper number 95GL00816  
0094-8534/95/95GL-00816\$03.00

**Table 1.** Latitude, Longitude, Elevation and Period of Record for the Radar Profiler Sites.

Site	lat (°N)	long (°W)	elevation (m MSL)	pd of record
Haviland, KS (HAV)	37.65	99.09	648	JFD 91 JF 92
Hudson, MA (HUD)	42.41	71.48	93	JFD 91 JF 92
Platteville, CO (PLT)	40.18	104.72	1524	JFD 91 JF 92

The basic data set at each site is composed of the time series of hourly wind vectors at each range gate for the entire period of record. The first step in the analysis was to produce a composite day for each of the sites, as illustrated for the Platteville site in Figure 2. In this composite day each of the vectors (i.e., for each hour and range gate) was determined by vector averaging all available winds for that hour and range gate for the entire period of record. Because signal-to-noise ratios decrease with radar range and a "consensus" algorithm requires consistent multiple wind determinations on each beam before a valid hourly wind can be reported, the number of hourly winds going into the vector average for the climatological day generally decreases with height, as shown in Figure 3, reducing the statistical significance of data from the upper range gates. The number of valid hourly wind observations does not vary greatly with time of day for the wintertime data utilized in our analyses so that Figure 3 is generally representative of all hours of the day. Once the composite days were constructed, harmonic analyses (Stull, 1988) were performed on the eastward-directed (u) and northward-directed (v) components of the 24 vector winds at each range gate for the composite day and the amplitudes and phases of the diurnal, semidiurnal and other harmonics were determined.

The pre-processing of the original hourly data into a composite day plays an important role in the analysis, as it provides an implicit bandpass filter that passes the diurnal signal and its harmonics while filtering out longer and shorter



Figure 1. Radar profiler locations.

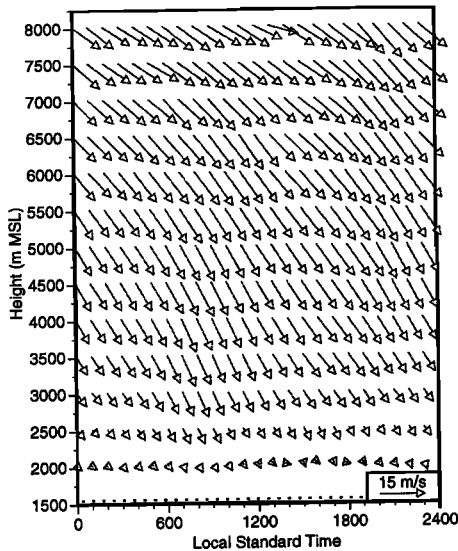


Figure 2. Mean daily time-height cross section of horizontal vector winds at Platteville, Colorado. Every other range gate is plotted. Vectors pointing to the right are blowing from the west, vectors pointing up are blowing from the south, etc.

period signals whose phases change from day to day. Thus, for example, passing synoptic-scale weather systems, which generally have a wind amplitude greater than the harmonic amplitudes being sought, are effectively filtered if the period of record is sufficiently long that enough events of different phase are sampled. Both local and global diurnal and harmonic circulations are passed by this filter.

It is well-known that any well-behaved continuous function can be described by an infinite Fourier series – in other words, by the sum of an infinite number of sine and cosine terms. In a case of a discrete time series with a finite number of points, however, only a finite number of sine and cosine terms are required to fit the points exactly. For a total of  $N$  data points in a period  $T$ , the highest frequency that can be resolved by discrete Fourier transforms is  $N/2$  waves. In our analyses,  $T$  is 24 hours, and the number of points,  $N$ , is 24 so that 12 (i.e.,  $N/2$ ) harmonic components with frequencies between 1 and 12 waves per day can fit the 24 hourly data points exactly.

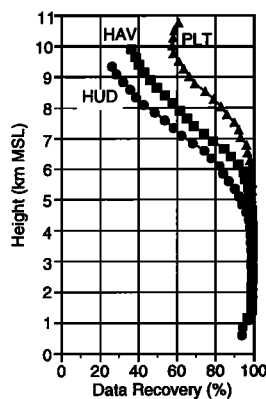


Figure 3. Percentage of valid wind measurements as a function of height. The number of possible hourly wind profiles is 2451 at HAV, 2798 at HUD, and 2486 at PLT.

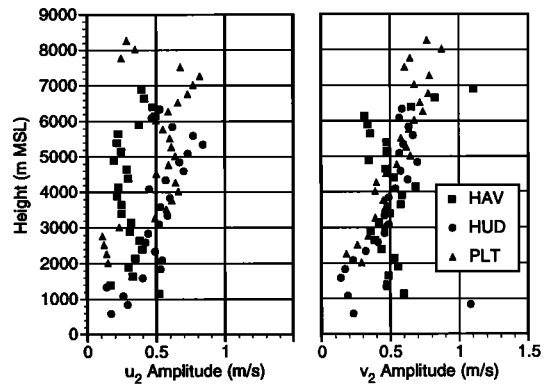


Figure 4. Semidiurnal wind component amplitudes as a function of height.

Here, we focus entirely on the semidiurnal harmonic component for the three stations, presenting the results in terms of amplitude (Figure 4) and phase (Figure 5) variations with height, and providing hodographs of the sum of the daily mean ( $u_0, v_0$ ) and semidiurnal ( $u_2, v_2$ ) harmonic components (Figure 6). Data are plotted only to altitudes where data recovery remained above 75% (6898 m MSL at HAV, 6343 m at HUD, and 8274 m at PLT).

The semidiurnal  $u$ - and  $v$ -component amplitudes (Figure 4) are weak near the ground, but increase with height to attain 0.5-0.7 m/s at altitudes between 5000 and 7000 m MSL. Figure 5 shows the phase of the semidiurnal oscillations represented in terms of the apparent local solar times (ALST) of the  $u$  and  $v$  wind component maxima (ALST is defined in Section 3). Above the first few range gates, the times of the individual component maxima are quite consistent between sites – the  $u$ -component maxima occurring at about 0400 (and 1600), and the  $v$ -component maxima occurring at about 0100 (and 1300) ALST. The semidiurnal wind turns clockwise with time, and because the two semidiurnal components are 90° out of phase and of approximately equal amplitude, hodographs (Figure 6) of the semidiurnal components are approximately circular.

### 3. Analytical Model of the Semidiurnal Solar Tide

Chapman and Lindzen (1970) developed an analytical model for semidiurnal tidal winds by solving perturbation equations for atmospheric motion on a rotating spherical earth with no

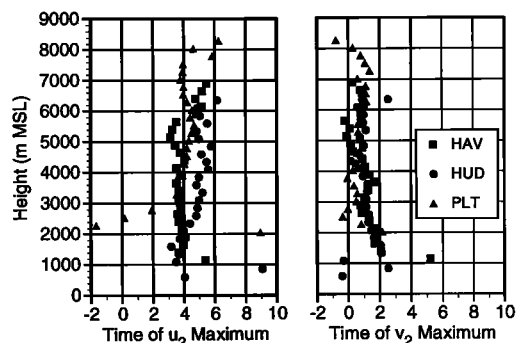


Figure 5. Semidiurnal wind component phases as a function of height. Times are Apparent Local Solar Time.

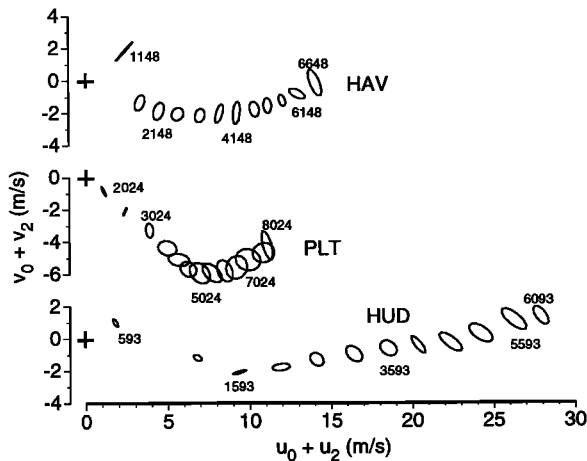


Figure 6. Hodograms of the sum of the mean daily and mean hourly semidiurnal wind components at every other range gate at the three sites. Labels at individual range gates are heights in meters MSL. The elliptical wind figure for each range gate is made up of 24 hourly points, each of which can be thought of as defining the tip of a wind vector drawn from the coordinate origin, indicated for each site by a plus sign. This vector rotates clockwise twice per day around each of the wind figures.

friction. The equations are driven by perturbation semidiurnal horizontal pressure gradient components, which are obtained by differentiating Haurwitz's (1956) analytical expression for the global semidiurnal surface pressure perturbation, as obtained by fitting analyzed data from 296 global barometric stations. His equation is

$$p = p_s \cos^3 \theta \sin[2(t' + \phi) + \sigma] \text{ hPa} \quad (1)$$

where  $p_s$  is the amplitude of the semidiurnal pressure oscillation at the equator (1.16 hPa),  $\theta$  is latitude,  $t'$  is Universal Time (UT) reckoned in angle at the rate of 360° per mean solar day from lower transit (i.e., midnight),  $\phi$  is east longitude, and  $\sigma$  is the initial phase of the pressure perturbation (158°). The solutions to Chapman and Lindzen's (1970) equation for the eastward and northward semidiurnal wind components, respectively, are

$$\begin{aligned} u &= C_s (1 + 1.5 \sin^2 \theta) \sin(2t'' + \sigma + 180^\circ) \\ v &= 2.5 C_s \sin \theta \sin(2t'' + \sigma + 90^\circ) \end{aligned} \quad (2)$$

where  $C_s = p_s / \rho R_E \Omega \approx 0.2 \text{ m/s}$ ,  $\rho$  is air density,  $R_E$  is the earth's radius,  $\Omega$  is the angular velocity of the earth,  $t'' = t' + \phi$  is apparent local solar time.

Minor differences between (2) and Chapman and Lindzen's (1970) published solution are due to their use of a  $v$  axis that points toward the south. Since Haurwitz's equation represents the semidiurnal pressure oscillation at the earth's surface, and the momentum equations apply only for a frictionless atmosphere, we make the additional assumption that the amplitude and phase of the semidiurnal pressure perturbation do not vary through the depth of the earth's frictional boundary layer. Then the solution can be considered valid at the top of the earth's frictional boundary layer.

From (2), the  $u$  and  $v$  components are, respectively, 180° and 90° out of phase with the pressure oscillation. The two wind components are in quadrature and are of approximately

equal amplitude poleward of 20°N (at 40° N, the mean latitude of the three profilers, the amplitudes are both 0.32 m/s), and the wind vector  $V = u i + v j$  rotates clockwise on a near-circular path twice per day. At the equator the winds have no  $v$ -component. The north wind component maxima are attained at 0044 and 1244 hr in the Northern Hemisphere, but at 0644 and 1844 in the Southern Hemisphere. The east wind component maxima are attained at 0344 and 1544 hr in both hemispheres.

#### 4. Discussion

The observed wind characteristics above the first few range gates generally match the characteristics of semidiurnal solar tidal wind oscillations predicted by the simple dynamic model. These observed characteristics include the global extent of the phenomenon, the oscillation frequency, the direction of rotation, the amplitude, and the phase.

The shallow near-ground layer for which the tidal phases do not match the phases predicted by the dynamical model is tentatively identified as the earth's frictional boundary layer. For our wintertime data this layer is about 850 m deep at HAV, 1150 m deep at HUD, and 1300 m deep at PLT, in general agreement with estimates of frictional boundary layer depths (e.g., Stull, 1988). Phase discrepancies in this layer may be caused by frictional effects or by the formal fitting of Fourier components to the strong diurnal oscillations in this layer during a season when the daytime and nighttime periods are of unequal length.

Key features of our observations, the phase itself and the near-constancy of the phase with altitude, agree with predictions of dynamic models in which the tidal oscillations are driven directly by ozone and water vapor absorption (e.g., Forbes, 1982; Miyahara et al., 1993), with Williams et al.'s (1992) equatorial radar profiler data, and with Wallace and Tadd's (1974) rawinsonde-derived tidal observations. Wallace and Tadd's observations were obtained from the global upper air sounding network during a period when four rawinsondes were flown per day at selected stations operated by the U.S. and New Zealand, and were apparently the first measurements from which semidiurnal tropospheric tidal characteristics could be inferred. Their technique did not have the time resolution necessary to isolate the semidiurnal tides from higher frequency harmonics, and to estimate the tidal amplitudes they assumed that the semidiurnal wind vector would rotate uniformly in a roughly circular pattern over the course of a day – an assumption that is supported by Figure 6.

The increase of semidiurnal tidal amplitudes with height in the troposphere, while consistent with the findings of Wallace and Tadd (1974), does not agree with model predictions (Forbes, 1982), or with recent equatorial data (Williams et al., 1992) obtained from a 50 MHz profiler at Christmas Island (2°N, 157°W) which showed small tidal  $u$ -component amplitudes (0.1 to 0.2 m/s) that were nearly invariant with height. Because Christmas Island is near the equator, from (2), the semidiurnal tidal  $v$ -component was small and could not be measured.

Figures 3 and 4 show differences in tidal phase and amplitude among the three North American sites. To evaluate the significance of differences between sites it is necessary to estimate the errors involved in individual determinations of phase and amplitude. An estimate of amplitude errors at individual sites can be made by assuming that the semidiurnal phase is given by the dynamical model in Section 2, and that

this phase is independent of height (see references above). Then, measured deviations from the predicted phase  $\delta P$  can be used to estimate tidal amplitude errors  $\delta A$  using the equation  $\delta A = A \sin \delta P$  (Chapman and Lindzen, 1970). When this method is applied to 6 months of hourly data at the three sites we find that, except for the lowest 3 or 4 range gates and for the highest few range gates where significant amounts of data are missing, radar profiler amplitude errors are generally between 0.05 and 0.2 m/s. The u-component amplitude errors at the HUD site, however, attain 0.4 m/s, possibly because the small semidiurnal tidal signal is difficult to separate from the "noise" introduced by strong west wind oscillations associated with the polar front jet, or due to actual tidal phase changes near the coast (Spar, 1952). We conclude from this analysis that longer periods of record are necessary before unambiguous determinations can be made of phase and amplitude differences between sites. Confidence ranges of less than 0.04 m/s were calculated from 4-yr data sets by Williams et al. (1992), suggesting that radar profiler data can provide the measurement accuracy required for this analysis.

## 5. Conclusions

A climatological analysis of hourly data from radar wind profilers at three sites in North America has identified a semidiurnal wind system in the mid-latitude troposphere. The wind system can be identified by first computing mean vector winds over the period of record for each hour of the day at individual radar range gates, and then performing harmonic analyses of the 24 wind components at each range gate. This procedure filters out nonharmonic oscillations such as those produced by traveling synoptic weather disturbances and does not require the original time series to be continuous (i.e., some missing data are allowed).

Because the semidiurnal wind system is seen at all sites, is regular, follows the apparent motion of the sun, turns clockwise with time, and has the approximate phases predicted by a dynamic model driven by the well-known semidiurnal tidal pressure gradient observed over the earth's surface, it is identified as a semidiurnal atmospheric solar tide. The tidal amplitude of 0.2-0.3 m/s at the top of the frictional boundary layer agrees with the predicted amplitudes there, but the observations show that this amplitude increases with height to attain 0.5-0.7 m/s at 5-7 km. At the 5-7 km heights, the observed amplitudes exceed tidal model predictions and equatorial site observations by more than a factor of two. The tidal phases are consistent from site to site and change little with altitude at the three sites investigated.

We plan to conduct further analyses of the variation of tidal characteristics with height, location, and season using

additional 915-, 404-, and 50-MHz radar profilers and longer periods of record.

**Acknowledgments.** The radar data were collected by the NOAA Forecast Systems Laboratory's Wind Profiler Demonstration Network and were supplied by Dr. Ray Arritt of Iowa State University. Mr. Dan Wolfe and Dr. Jim Wilczak of the NOAA Environmental Technology Laboratory are thanked for useful discussions on radar profiler operation.

Research was supported by the U.S. Department of Energy under Contract DE-AC06-76RLO 1830 at Pacific Northwest Laboratory as part of DOE's Atmospheric Studies in Complex Terrain and Atmospheric Radiation Measurements programs. Pacific Northwest Laboratory is operated for the DOE by Battelle Memorial Institute.

## References

- Chapman, S., and R. S. Lindzen, 1970: *Atmospheric Tides*. D. Reidel Publishing Co., Dordrecht, 200 pp.
- Doviak, R. J., and D. S. Zrnic, 1984: *Doppler Radar and Weather Observations*. Academic Press, 458 pp.
- Forbes, J. M., 1982: Atmospheric tides 2. The solar and lunar semidiurnal components. *J. Geophys. Res.*, 87, 5241-5252.
- Haurwitz, B., 1956: The geographical distribution of the solar semidiurnal pressure oscillation. *Meteor. Pap.*, 2(5), New York University.
- Miyahara, S., Y. Yoshida, and Y. Miyoshi, 1993: Dynamic coupling between the lower and upper atmosphere by tides and gravity waves. *J. Atmos. Terr. Phys.*, 55, 1039-1053.
- Strauch, R. G., D. A. Merritt, K. P. Moran, K. B. Earnshaw, and D. van de Kamp, 1984: The Colorado wind profiling network. *J. Atmos. Oceanic Technol.*, 1, 37-49.
- Stull, R. B., 1988: *An Introduction to Boundary Layer Meteorology*. Kluwer Academic Publishers, Dordrecht, 666 pp.
- Wallace, J. M., and R. F. Tadd, 1974: Some further results concerning the vertical structure of atmospheric tidal motions within the lowest 30 kilometers. *Mon. Wea. Rev.*, 102, 795-803.
- Wilczak, J. M., R. G. Strauch, F. M. Ralph, B. L. Weber, D. A. Merritt, J. R. Jordan, D. E. Wolfe, L. K. Lewis, D. B. Wuertz, J. E. Gaynor, S. A. McLaughlin, R. R. Rogers, A. C. Riddle, and T. S. Dye, 1995: Contamination of wind profiler data by migrating birds: Characteristics of corrupted data and potential solutions. *J. Atmos. Oceanic Technol.*, in press.
- Williams, C. R., S. K. Avery, J. R. McAfee, and K. S. Gage, 1992: Comparison of observed diurnal and semidiurnal tropospheric winds at Christmas Island with tidal theory. *Geophys. Res. Lett.*, 19, 1471-1474.

C. D. Whiteman and Xindi Bian, Boundary Layer Meteorology Group, Battelle Northwest Laboratories, P. O. Box 999, Richland, WA 99352. (e-mail: cd\_whiteman@pnl.gov and x\_bian@pnl.gov)

(Received November 1, 1994; revised February 7, 1995; accepted February 17, 1995)